UC Berkeley
UC Berkeley Previously Published Works

Title

Dissolution of Lithium Metal in Poly(ethylene oxide)

Permalink

https://escholarship.org/uc/item/7f68t2fj

Journal

ACS Energy Letters, 4(4)

ISSN

2380-8195

Authors

Galluzzo, Michael D
Halat, David M
Loo, Whitney S
et al.

Publication Date

2019-04-12

DOI

10.1021/acsenergylett.9b00459

Peer reviewed

Dissolution of Lithium Metal in Poly(ethylene oxide)

Michael D. Galluzzo[1,2], David M. Halat[1,3], Whitney S. Loo[1], Scott A. Mullin[1], Jeffrey A. Reimer[1,2], and Nitash P. Balsara[1,2,3]*

[1]Department of Chemical and Biomolecular Engineering University of California, Berkeley, CA 94720, United States.

[2]Materials Science Division, Lawrence Berkeley National Laboratory, Berkeley, CA 94720, United States

[3]Joint Center for Energy Storage Research (JCESR), Lawrence Berkeley National Laboratory, Berkeley, CA 94720, United States.

AUTHOR INFORMATION

Corresponding Author

* Correspondence to: nbalsara@berkeley.edu

ABSTRACT

We demonstrate that lithium metal is sparingly soluble in poly(ethylene oxide) (PEO). ^{7}Li NMR shows that when a PEO sample is placed in contact with lithium metal at elevated temperatures, a lithium species dissolves and diffuses into the bulk polymer. A lithium/PEO/lithium electrochemical cell, containing no lithium salts, shows increasing

conductivity over time when annealed at 120 °C. Chronoamperometry shows that the annealed

cell obeys Ohm's law, implying that conduction occurs without the development of concentration

gradients. To explain the results, it is proposed that atomic lithium dissolves into PEO, where it

exists as a lithium cation and free electron. The dissolution of lithium also affects the phase

behavior of block copolymer electrolytes. These observations explain the strong adhesion between

lithium metal and PEO and have important implications for lithium metal battery systems that

contain PEO-based electrolytes.

TOC GRAPHICS
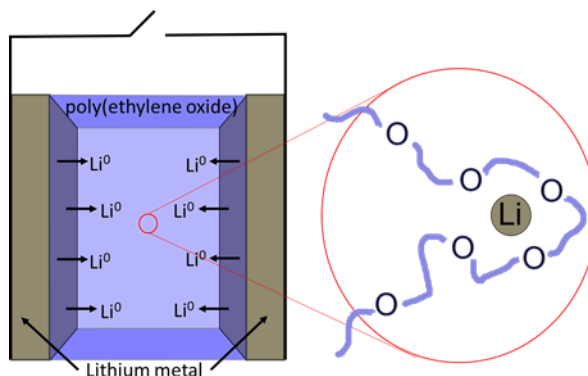
MAIN TEXT

Rechargeable batteries containing a lithium metal anode will provide the next step towards

more efficient energy storage compared to today's lithium ion batteries[1]. While lithium metal

batteries were once produced commercially, several issues resulted in their retraction from the

market place. Organic liquid electrolytes currently used in lithium-ion batteries cannot be used in

cells with lithium metal anodes due to dendrite formation, irreversible parasitic reactions at the

lithium-electrolyte interface, and the increased likelihood that a short circuit will ignite the

flammable electrolyte[2,3]. Solid electrolytes provide an attractive option to enable lithium metal anodes[4].

Salt-doped poly(ethylene oxide) (PEO) has been studied extensively due to its potential to enable rechargeable batteries with lithium metal anodes[5–8]. Mixtures of PEO and salt exhibit reasonable conductivities at temperatures above the melting point of PEO. PEO-based solid electrolytes can be prepared by adding salts to a block copolymer comprising a PEO block and a mechanically rigid block such as polystyrene (PS). A remarkable property of the interface between PEO-based electrolytes (both homopolymers and block copolymers) and lithium metal is the observation that good mechanical and electrical contact are maintained even when tens of micrometers of lithium are displaced during cycling[9,10]. Rigid, inorganic solid electrolytes (ceramics and glasses) have also been used to stabilize the lithium metal anode but are limited by high interfacial resistance and require large applied pressures[11]. In contrast, cells with polymer electrolytes and lithium metal anodes cycle with no applied pressure[12]. In spite of extensive studies[13,14], the nature of the PEO-lithium interface is not well understood.

We report herein a simple observation that provides fresh insight into the nature of the PEO-lithium interface: lithium metal is sparingly soluble in PEO. Primary evidence comes from [7]Li nuclear magnetic resonance (NMR) spectroscopy. In addition, we present the signatures of lithium dissolution in electrochemical cells as well as changes in the thermodynamic properties of a PEO-containing block copolymer electrolyte. To our knowledge, this is the first report of metal solubility in a polymer.

A cell comprising two lithium foils sandwiched around a 2 mm thick PEO sample was sealed in an aluminum laminated pouch and placed in an oven at 130 °C. After 12 days, the sample was removed from the oven, cooled to room temperature, and brought into the glovebox

to remove the lithium foils. Lithium metal adheres strongly to PEO. A razor blade was used to extract a slice of the polymer from the middle of the cell (taking care to exclude the lithium foils). We performed this experiment on three PEO samples with molecular weights 5, 35, and 275 kg mol^{-1}.

The PEO sample was placed in a 3.3 mm NMR tube and inserted into a 5 mm tube designed for a coaxial sample configuration. The outer compartment was then filled with a solution of bis(trifluoromethylsulfonyl)amine lithium salt (LiTFSI) in tetraglyme with known salt concentration. The mass of the PEO sample and the LiTFSI/tetraglyme solution was roughly 50 mg each. The entire coaxial sample was sealed with a hermetic cap and removed from the glovebox. Variable temperature ^{7}Li NMR was performed at 90 °C using a Bruker Avance III 600 MHz spectrometer. (For the purpose of the NMR experiment, it is only important that the sample temperature be above the melting temperature of PEO.) The ^{7}Li NMR spectra are plotted as open circles for 5, 35, and 275 kg mol^{-1} in Figures 1a-c.

In Figure 1a (5 kg mol^{-1} PEO), we see two peaks in the spectrum; a broad peak at approximately 1.5 ppm and a sharper peak at -0.2 ppm. NMR spectra from samples without the reference solution only showed a broad peak at 1.5 ppm (see Figure S1a). The sharp peak is attributed to the LiTFSI in tetraglyme. We note in passing that the NMR signature of lithium metal is a peak at 260 ppm[15]. In order to deconvolute the integrated intensity of the two peaks in Figure 1a, we fit the broad peak to a Lorentzian function and the sharp peak to a Gaussian function. The combined fit is shown as a red line in Figure 1a. We then obtained the integrated intensity for each peak and compare them to solve for the lithium concentration (in molality, m) in the PEO sample (see details of calculation in Supporting Information). Qualitatively similar results are obtained for 35 and 275 kg mol^{-1} PEO in Figures 1b-c annealed at 130 °C. While the

dependence on the dissolution process with annealing temperature remains to be determined, we have observed qualitatively similar results (i.e. NMR signatures of a solvated lithium species) in samples annealed for a variety of annealing times and at annealing temperatures ranging from 90 °C to 140 °C.
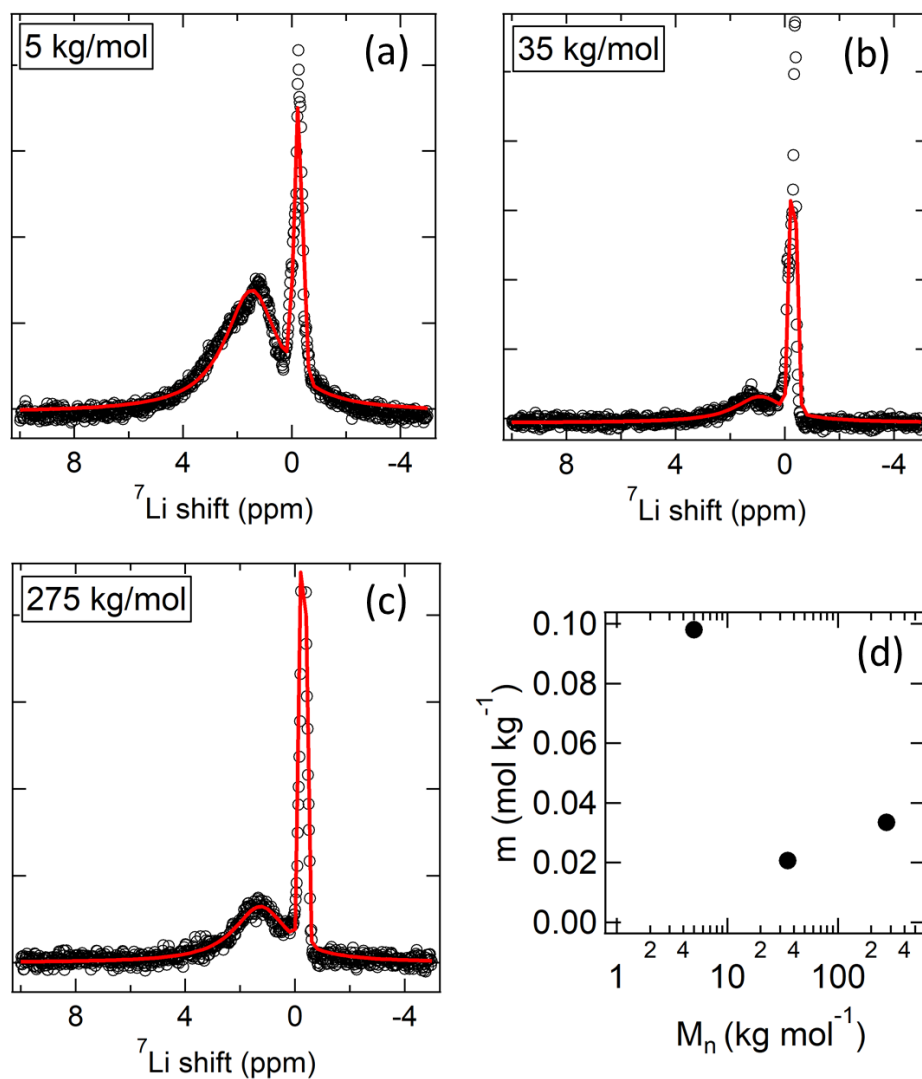

Figure 1. ^{7}Li NMR spectra (open circles) of (a) 5 kg mol^{-1} (b) 35 kg mol^{-1} and (c) 275 kg mol^{-1} PEO annealed against lithium metal for 12 days at 130 °C in a coaxial NMR tube with a reference solution in the outer compartment. Red lines are fits to the experimental data. (d) Lithium molality as a function of

PEO molecular weight calculated by comparing peak integrations from the lithium in the PEO sample to the reference.

Figure 1d shows the lithium concentration in molality as a function of PEO molecular weight. In 5 kg mol⁻¹ PEO, the molality of lithium is 0.1 mol kg⁻¹. We note that a typical PEO/LiTFSI electrolyte will have an LiTFSI molality between 1.0 and 2.0 mol kg⁻¹. When the molecular weight is increased to 35 kg mol⁻¹, we observe a decrease in the lithium concentration by a factor of about 5. The lithium concentration in the 275 kg mol⁻¹ sample is similar to that in the 35 kg mol⁻¹ sample. If the dissolution mechanism was facilitated by a reaction with the hydroxy end groups, we would expect the lithium concentration to be proportional to the molecular weight. This suggests that the lithium dissolution occurs due to an interaction with the ether backbone of the polymer chain. Gel permeation chromatography (GPC) and Fourier transform infrared spectroscopy (FTIR) experiments on the PEO/Li mixtures (presented in Figure S2 and S3, respectively) indicate that the PEO chains are not degraded by the dissolution process.

To further characterize the solvated lithium species, we assembled lithium/PEO/lithium cells and performed electrochemical impedance spectroscopy while annealing them at 120 °C. The thickness of the PEO layer (L) was 275 μm. Figure 2a shows representative Nyquist plots for the 35 kg mol⁻¹ PEO sample over the course of 7 days at 120 °C. The diameter of the semicircle presented in the Nyquist plot is a measure of the overall resistance of the PEO layer. Pure PEO conducts neither electrons nor ions, and at early times (less than 1 day), the Nyquist plot indicates a resistance of 100 kΩ cm². We attribute this to the presence of ionic impurities with the PEO. The diameter of the Nyquist semicircle decreases significantly after two days of annealing, and it reaches a plateau after seven days. The data in Figure 2a can be used to calculate conductivity, κ,

as a function of time (see details in Supporting Information). The results are shown in Figure 2b. Over the timescale of seven days, κ increases by a factor of 16. We attribute this increase to the dissolution of lithium species in PEO. We also performed a control experiment wherein PEO was sandwiched between stainless steel electrodes at 120 °C. The result of this experiment is shown in Figure 2b. In the control experiment, κ is more-or-less independent of time in the window between 2 hours and 7 days. The finite conductivity measured in the control experiment is attributed to impurities. It is clear that contacting PEO with lithium metal results in the dissolution of lithium species that contribute to conductivity.
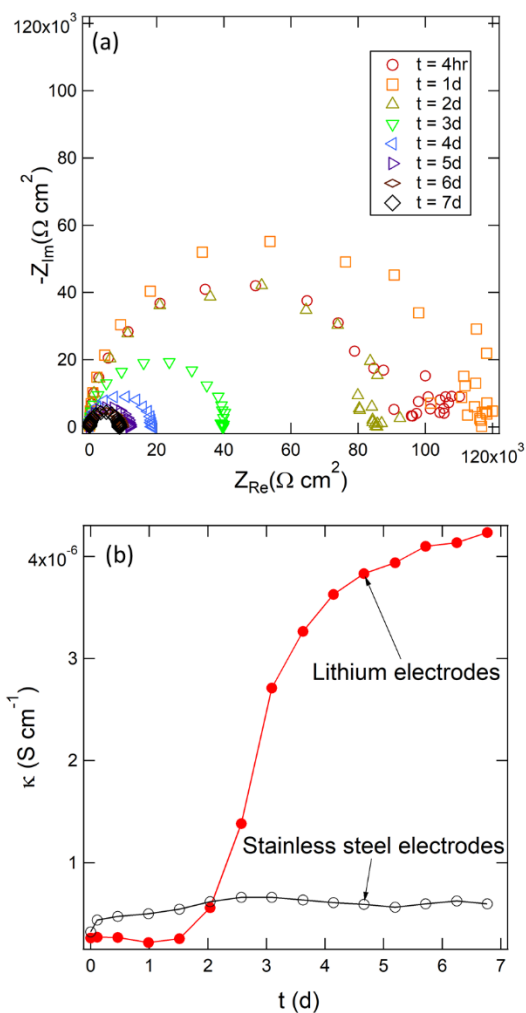
Figure 2. (a) Representative series of Nyquist plots obtained from a lithium/35 kg mol^{-1} PEO/lithium cell annealed at 120 °C over the course of 7 days. (B) Conductivity, κ, of a lithium/35 kg mol^{-1} PEO/lithium (closed symbols) and stainless steel/35 kg mol^{-1} PEO/stainless steel cell (open symbols) as a function of time at 120 °C.

Figure 3 presents the results of a dc polarization experiment on a lithium/PEO/lithium cell (L = 500 μm). The cell, containing 35 kg mol^{-1} PEO, was annealed at 120 °C for 10 days and the resulting Nyquist plot is shown in Figure 3a. The resistance of the PEO with dissolved lithium species is 5.7 kΩ cm^2 at this point. A constant potential, Φ, of 19 mV was applied to the cell and the resulting current density, i, as a function of time is shown in Figure 3b. When lithium salts are

dissolved in PEO, a gradual decrease in i is typically observed due to the development of salt concentration gradients[16,17]. In contrast, i is independent of time in Figure 3b. This is the characteristic of conduction in samples without concentration gradients, e.g. a single-ion conductor[18,19]. In the absence of concentration gradients, i can be calculated using Ohm's law. The calculated i, 3.3 μA cm^{-2}, is similar to the measured value of 3.4 μA cm^{-2}. After imposing $\Phi = 19$ mV across the cell for 66 min, the current was set to zero and the resulting Φ (i.e. the open circuit potential) was monitored as a function of time. The result is shown in Figure 3c where we see that the open circuit potential drops instantaneously to zero. This is also a property of conductors without concentration gradients. The dissolved lithium species thus enable conduction in PEO without the introduction of concentration gradients.
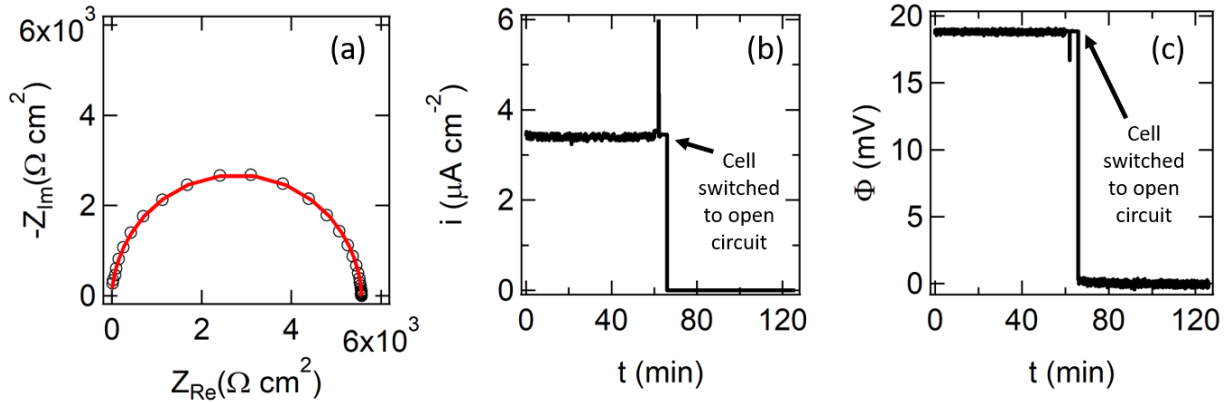

Figure 3. Electrochemical data from a chronoamperometry experiment preformed on a Li/35 kg mol^{-1} PEO/Li cell after being annealed at 120 °C for 10 days. (a) Nyquist plot (open circles) from ac impedance spectroscopy performed before polarization. The cell resistance is obtained by fitting to an equivalent circuit (red line). (b) Current density, i, measured in response to a 19 mV polarization. i is set to zero at $t = 66$ min. (c) Cell potential, Φ, monitored over the course of the experiment. At $t = 66$ min, the cell is set to open circuit (i.e. $i = 0$). The applied potential was momentarily interrupted at $t = 60$ min, resulting in the spike observed in (b) and (c).

We posit that the dissolved lithium species in PEO comprise a lithium cation and free electron. It is well known that alkali metals are soluble in polar solvents such as ammonia and

cyclic ethers; indeed the solubility of lithium metal in ammonia has been known for over a century[20]. These mixtures are highly reactive electron conductors. While there are many reports of dissolving sodium and potassium in cyclic ethers[21–24], the possibility of dissolving lithium in ethers has, to our knowledge, not been reported. Additional work is required to establish the properties of lithium metal dissolved in PEO. Recent work has shown that electrical conductivity can be obtained in a radical-containing polymer[25]. The observed conduction in PEO with dissolved lithium could be due to the mobility of lithium cations, free electrons, or both.

Block copolymers exhibit a reversible order-to-disorder transition, and dissolving salts is known to stabilize the ordered phase[26–28]. In particular, the addition of LiTFSI to polystyrene-*block*-polyethylene oxide (SEO) results in an increase in the order-to-disorder transition temperature (T_{ODT})[29]. Figure 4a presents a phase diagram of an SEO block copolymer with a PS molecular weight of 1.7 kg mol^{-1} and PEO molecular weight of 1.4 kg mol^{-1} reproduced from ref 29. (The molecule is terminated by a sec butyl group and a hydroxy group on the PS and PEO ends, respectively.) The system exhibits a disordered phase at low salt concentrations and an ordered lamellar phase at high salt concentrations. The T_{ODT} of SEO/LiTFSI mixtures is plotted as a function of salt molality, *m*, in Figure 4a.
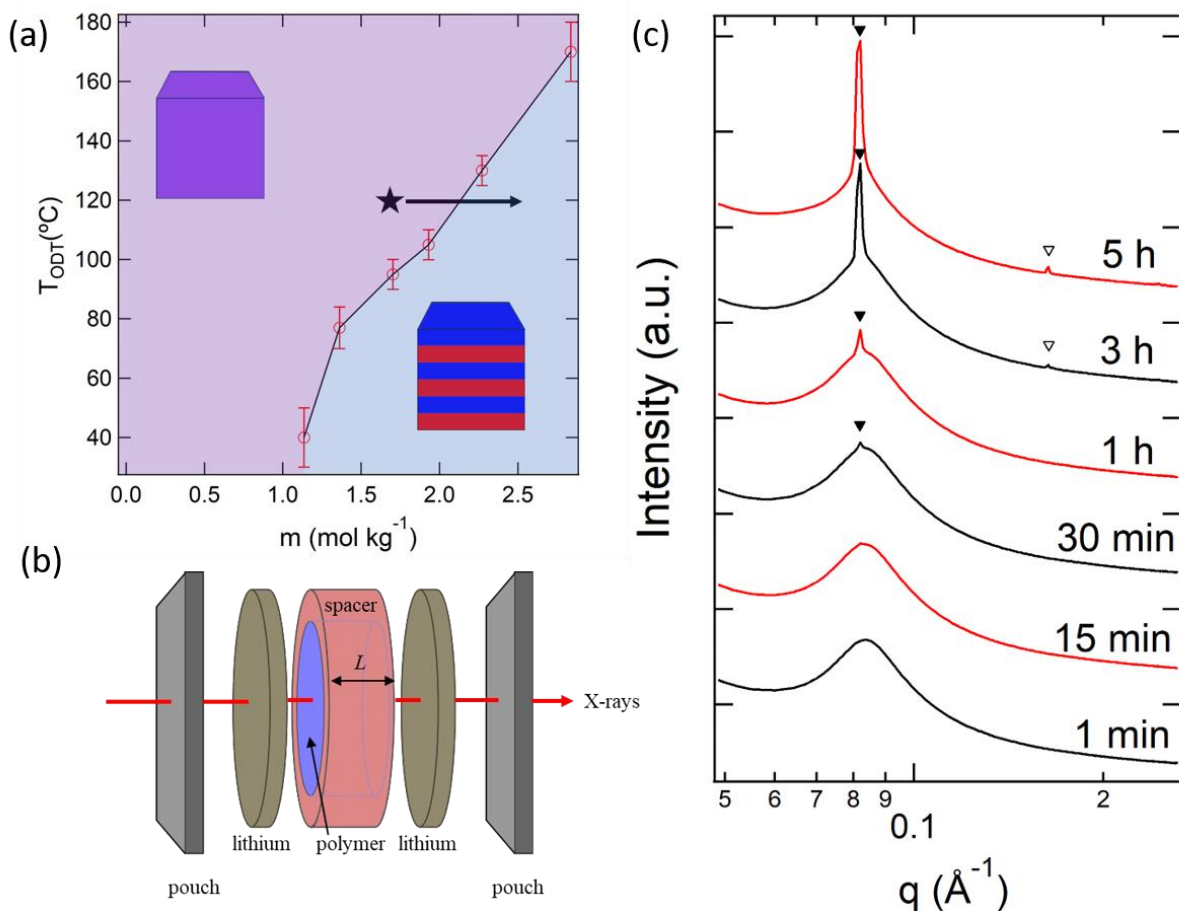
Figure 4. (a) Order-to-disorder transition temperature (T_{ODT}) of the SEO/LiTFSI mixture as a function of LiTFSI molality, m, denoted by open circles[29]. (b) Sample configuration for the SAXS experiments, indicating the orientation of the X-ray beam. (c) SAXS profiles of the SEO/LiTFSI mixture as a function of time. Filled and open triangles indicated the appearance of a primary and secondary scattering peak at q^* and $2q^*$, respectively.

We sandwiched an SEO/LiTFSI mixture with $m = 1.70$ mol kg^{-1} and $L = 380$ μm between two lithium windows and studied the morphology of this mixture as a function of time at 120 °C using small angle X-ray scattering (SAXS). At equilibrium (i.e. with inert windows), this sample is disordered and the filled star in Figure 4a indicates the position of this sample on the phase diagram. All SAXS measurements were performed at beamline 7.3.3. of the Advanced Light Source (ALS) at Lawrence Berkeley National Laboratory[30] and data was reduced using the Nika program for IGOR Pro[31]. The sample geometry is shown schematically in Figure 4b. X-rays are

passed perpendicular to the lithium windows. The time dependent SAXS profiles thus obtained are shown in Figure 4c.

At early times, the SAXS profile contains a broad scattering peak which is a standard signature of disordered concentration fluctuations[32]. This is not surprising, as the mixture is 25 °C above the T_{ODT}. However, the emergence of a sharp scattering peak superimposed on the broad peak after 15-30 minutes indicates the presence of an ordered phase. As time proceeds, the sharp peak grows at the expense of the disordered peak. After 5 hours, the sample is nearly completely ordered as indicated by a sharp primary peak at $q = q^*$. The second order peak at $q = 2q^*$ confirms that the ordered phase is lamellar. A control experiment was performed using aluminum windows. The resulting SAXS profiles were independent of time with a scattering profile characteristic of a disordered morphology (see Figure S4). Qualitatively similar results are shown for a higher molecular weight SEO polymer with no lithium salts added. A disorder-to-order transition occurs at a temperature greater than 40 °C above the T_{ODT} when placed in contact with lithium metal (see Figure S5). The SAXS data in Figure 4c and S5 indicate that the lithium species that dissolves into the SEO copolymer (with or without LiTFSI present) stabilizes the ordered phase. The arrow in Figure 4a qualitatively depicts this phenomenon. This result is consistent with the phenomena observed when neat PEO is placed against lithium metal and confirms that the lithium dissolution process occurs in both homopolymer and block copolymers.

In summary, we have shown that when PEO-containing polymers are placed against lithium metal, lithium ions along with the associated electrons dissolve into the polymer. This dissolved species is shown to affect the conductivity of the polymer as well as the thermodynamics of block copolymer systems. These results have important implications for battery systems containing lithium metal and any PEO-based material. On one hand, the dissolution of lithium

metal may be problematic and lead to decreased coulombic efficiency. On the other hand, it may explain why PEO-containing polymers exhibit strong adhesion to lithium metal, even in the case of block copolymers with high elastic moduli. Future work will be directed at characterizing the chemical environment of the solvated lithium, determining the solubility limit, and studying the dissolution process when a lithium salt is present.

ASSOCIATED CONTENT

Supporting Information. Materials, sample preparation, experimental details, fitting of NMR data and Nyquist plots, NMR spectra of lithium dissolved in 35 kg mol^{-1} PEO with hydroxy end groups and 2 kg mol^{-1} PEO with dimethyl ether end groups annealed at 90 °C, GPC and FTIR of 35 kg mol^{-1} with dissolved lithium, time dependent SAXS profiles of an SEO/LiTFSI mixture annealed at 120 °C against aluminum windows, time dependent SAXS profiles of a salt-free SEO block copolymer annealed at 120 °C against lithium windows showing a disorder-to-order transition.

AUTHOR INFORMATION

Corresponding Author

*E-mail: nbalsara@berkeley.edu

Notes

The authors declare no competing financial interest.

REFERENCES

(1)   Lin, D.; Liu, Y.; Cui, Y. Reviving the Lithium Metal Anode for High-Energy Batteries. *Nat. Nanotechnol.* **2017**, *12* (3), 194–206.

(2)   Tarascon, J.-M.; Armand, M. Issues and Challenges Facing Rechargeable Lithium Batteries. *Nature* **2001**, *414*, 359-367.

(3)   Tikekar, M. D.; Choudhury, S.; Tu, Z.; Archer, L. A. Design Principles for Electrolytes and Interfaces for Stable Lithium-Metal Batteries. *Nat. Energy* **2016**, *1* (9), 16114.

(4)   Long, L.; Wang, S.; Xiao, M.; Meng, Y. Polymer Electrolytes for Lithium Polymer Batteries. *J. Mater. Chem. A.* **2016**, *4*, 10038-10069.

(5)   Fenton, D. E.; Parker, M.; Wright, P. V. Complexes of Alkali Metal Ions with Poly(Ethylene Oxide). *Polymer* **1973**, *14*, 589.

(6)   Teran, A. A.; Tang, M. H.; Mullin, S. A.; Balsara, N. P. Effect of Molecular Weight on Conductivity of Polymer Electrolytes. *Solid State Ionics* **2011**, *203*, 18–21.

(7)   Lascaud, S.; Perrier, M.; Vallee, A.; Besner, S.; Prud'homme, J.; Armand, M. Phase Diagrams and Conductivity Behavior of Poly(Ethylene Oxide)-Molten Salt Rubbery Electrolytes. *Macromolecules* **1994**, *27* (25), 7469–7477.

(8)   Pesko, D. M.; Timachova, K.; Bhattacharya, R.; Smith, M. C.; Villaluenga, I.; Newman, J.; Balsara, N. P. Negative Transference Numbers in Poly(Ethylene Oxide)-Based Electrolytes. *J. Electrochem. Soc.* **2017**, *164* (11), E3569–E3575.

(9)   Stone, G. M.; Mullin, S. A.; Teran, A. A.; Hallinan, D. T.; Minor, A. M.; Hexemer, A.; Balsara, N. P. Resolution of the Modulus versus Adhesion Dilemma in Solid Polymer Electrolytes for Rechargeable Lithium Metal Batteries. *J. Electrochem. Soc.* **2012**, *159* (3), A222–A227.

(10)   Zhang, Q.; Liu, K.; Ding, F.; Liu, X. Recent Advances in Solid Polymer Electrolytes for Lithium Batteries. *Nano Res.* **2017**, *10* (12), 4139–4174.

(11)   Gao, Z.; Sun, H.; Fu, L.; Ye, F.; Zhang, Y.; Luo, W.; Huang, Y. Promises, Challenges, and Recent Progress of Inorganic Solid-State Electrolytes for All-Solid-State Lithium Batteries. *Adv. Mater.* **2018**, *30* (17), 1705702.

(12)   Zeng, H.; Ji, X.; Tsai, F.; Zhang, Q.; Jiang, T.; Li, R. K. Y.; Shi, H.; Luan, S.; Shi, D. Enhanced Cycling Performance for All-Solid-State Lithium Ion Battery with LiFePO4 Composite Cathode Encapsulated by Poly (Ethylene Glycol) (PEG) Based Polymer Electrolyte. *Solid State Ionics* **2018**, *320*, 92–99.

(13)   Fauteux, D. Lithium Electrode/PEO-Based Polymer Electrolyte Interface Behavior Between 60 and 120C. *J. Electrochem. Soc.* **1988**, *135* (9), 2231-2237.

(14)   Bouchet, R.; Lascaud, S.; Rosso, M. An EIS Study of the Anode Li/PEO-LiTFSI of a Li Polymer Battery. *J. Electrochem. Soc.* **2003**, *150* (10), A1385-A1389.

(15)   Carter, G. C.; Bennett, L. H.; Kahan, D. J. *Metallic Shifts in NMR : A Review of the Theory and Comprehensive Critical Data Compilation of Metallic Materials*; Pergamon Press: Oxford, UK, **1977**.

(16)   Doyle, M.; Newman, J. Analysis of Transference Number Measurements Based on the Potentiostatic Polarization of Solid Polymer Electrolytes. *J. Electrochem. Soc.* **1995**, *142* (10), 3465.

(17)   Evans, J.; Vincent, C. A.; Bruce, P. G. Electrochemical Measurement of Transference Numbers in Polymer Electrolytes. *Polymer (Guildf).* **1987**, *28* (13), 2324–2328.

(18)   Sun, X.-G.; Reeder, C. L.; Kerr, J. B. Synthesis and Characterization of Network Type Single Ion Conductors. *Macromolecules* **2004**, *37*(6), 2219-2227.

(19)   Zhang, H.; Li, C.; Piszcz, M.; Coya, E.; Rojo, T.; Rodriguez-Martinez, L. M.; Armand, M.; Zhou, Z. Single Lithium-Ion Conducting Solid Polymer Electrolytes: Advances and Perspectives. *Chem. Soc. Rev.* **2017**, *46* (3), 797–815.

(20)   Seely, C. On Ammonium and the Solubility of Metals without Chemical Action. *Chem. News* **1871**, *23* (594), 169–170.

(21)   Cafasso, F.; Sundheim, B. R. Solutions of Alkali Metals in Polyethers. I. *J. Chem. Phys.* **1959**, *31* (3), 809–813.

(22)   Panayotov, I. M.; Tsvetanov, C. B.; Berlinova, I. V.; Velichkova, R. S. Alkali Metal Solutions in Organic Solvents Obtained in the Presence of Polyethylene Oxide. *Die Makromol. Chemie* **1970**, *134* (1), 313–316.

(23) Jedlinski, Z.; Sokol, M. Solubility of Alkali Metals in Non-Aqueous Supramolecular Systems. *Pure Appl. Chem.* **1995**, *67* (4), 587–592.

(24) Dye, J. L. The Alkali Metals: 200 Years of Surprises. *Philos. Trans. R. Soc. A Math. Phys. Eng. Sci.* **2015**, *373* (2037), 20140174.

(25) Joo, Y.; Agarkar, V.; Sung, S. H.; Savoie, B. M.; Boudouris, B. W. A Nonconjugated Radical Polymer Glass with High Electrical Conductivity. *Science* **2018**, *359* (6382), 1391–1395.

(26) Ruzette, A.-V. G.; Soo, P. P.; Sadoway, D. R.; Mayes, A. M. Melt-Formable Block Copolymer Electrolytes for Lithium Rechargeable Batteries. *J. Electrochem. Soc.* **2001**, *148* (6), A537-A543.

(27) Young, W.-S.; Epps, T. H. Salt Doping in PEO-Containing Block Copolymers: Counterion and Concentration Effects. *Macromolecules* **2009**, *42* (7), 2672–2678.

(28) Thelen, J. L.; Teran, A. A.; Wang, X.; Garetz, B. A.; Nakamura, I.; Wang, Z. G.; Balsara, N. P. Phase Behavior of a Block Copolymer/Salt Mixture through the Order-to-Disorder Transition. *Macromolecules* **2014**.

(29) Mullin, S. A.; Stone, G. M.; Teran, A. A.; Hallinan, D. T.; Hexemer, A.; Balsara, N. P. Current-Induced Formation of Gradient Crystals in Block Copolymer Electrolytes. *Nano Lett.* **2012**, *12* (1), 464–468.

(30) Hexemer, A.; Bras, W.; Glossinger, J.; Schaible, E.; Gann, E.; Kirian, R.; MacDowell, A.; Church, M.; Rude, B.; Padmore, H. A SAXS/WAXS/GISAXS Beamline with Multilayer

Monochromator. *J. Phys. Conf. Ser.* **2010**, *247* (1), 012007.

(31)   Ilavsky, J.; IUCr. *Nika* : Software for Two-Dimensional Data Reduction. *J. Appl. Crystallogr.* **2012**, *45* (2), 324–328.

(32)   Leibler, L. Theory of Microphase Separation in Block Copolymers. *Macromolecules* **1980**, *13* (6), 1602–1617.